FORCES INDUCED ON A VERTICAL BREAKWATER BY INCIDENT OBLIQUE WAVES

Javier L. Lara [1], Pablo Higuera[1], María Maza [1], Manuel del Jesus[1], Iñigo J. Losada[1] and Gabriel Barajas[1]

Over the last years Navier-Stokes numerical models have been developed to accurately simulate wave interaction with all kinds of coastal structures, focusing on both functionality and stability of coastal structures. Although several models have been used to simulate wave interaction with coastal structures in two dimensions (2DV) there are a vast number of three-dimensional effects that need to be investigated in order to improve the design. In this paper a new model called IH-FOAM has been applied to study a vertical breakwater at prototype scale. As a first attempt of validation, the model has been used to simulate a regular wave train generated with a relative angle with the breakwater inducing three-dimensional wave patterns not only seaward the structure due to reflection but also generating an overtopping discharge variation along the breakwater trunk. Pressure laws and overtopping discharge at three different cross-sections along the structure have been studied. The pressure laws have been compared with classical Goda's formulation. Although, the numerical model predictions are in accordance with Goda's calculations, a clear three-dimensional variability of wave-induced pressure has been observed. Moreover, an additional study has been performed calculating pressure laws on the side-wall at the breakwater head. Large three-dimensional effects are detected from the simulations due to the flow separation at that area. Overtopping model predictions have been compared with Overtopping Manual calculations showing very close values along the trunk. However, lower overtopping discharge values are observed at the breakwater head. This paper is a preliminary work to show the range of applicability of a three-dimensional Navier-Stokes model to study wave interaction with a vertical breakwater under the action of an oblique wave train.

INTRODUCTION

The use of Navier-Stokes (NS) equations applied to coastal engineering processes is one of the main advances of the field over the last decade. There are several reasons to explain the increasing popularity of that approach. The increment of the computational resources and the improvement of the numerical aspects mainly related with the boundary conditions have made possible to excel the inherent limitations of classical depth averaged models. NS models overcome most of the simplifications behind wave theories. The highly non-linear and highly dispersive nature of the NS equations allows modeling complex wave transformation processes, as the ones that appear in the interaction of waves with coastal structures. Moreover, they do not require empirical formulations in order to trigger breaking and to determine the breakpoint location as on Boussinesq-type models.

As a first approach, two-dimensional Reynolds Averaged Navier-Stokes (RANS) models (Lara et al., 2008; Losada et al., 2008; Guanche et al., 2009) have revealed that structural functionality and stability can be studied with a high degree of accuracy, even in the presence of granular material layers. Volume-Averaged Reynolds-Averaged Navier-Stokes equations (VARANS) are solved to characterize wave induced flows within porous structures. Nowadays the computational cost is suitable to be applied to solve real problems. Numerical simulations are now possible to be long enough to provide reliable statistics regarding the functionality and stability magnitudes of coastal structures, such as mean overtopping discharge or wave induced forces. Nevertheless the fact that that most of them are 2D is a limiting factor. This involves that wave incidence must be normal to allow the comparison of results.

A qualitative progress is introduced with three-dimensional models (del Jesus et al., 2012; Lara et al., 2012; Higuera et al., 2013a,b). These are not so limited because they reproduce full 3D wave transformation processes, as diffraction, which typically occur on breakwater heads. Also oblique or fully directional wave trains can be generated to study the influence of the angle of incidence on the aforementioned variables. The purpose of this work is to test the capabilities of a fully three-dimensional CFD code based on N-S equations to solve the induced hydrodynamics of oblique waves around vertical breakwaters. In order to do so, a comparison between induced pressures on the caisson will be carried out, using Goda and Goda & Takahashi formulations.

The work is organized as follows. The numerical model is presented first. The numerical simulations are described next. Both wave induced pressure and overtopping discharge numerical results compared with traditional formulations are discussed in the following section. Finally some conclusions are presented.

---

[1] Environmental Hydraulics Institute "IH Cantabria", Universidad de Cantabria, C/ Isabel Torres no15, Parque Científico y Tecnológico de Cantabria, 39011, Santander, Spain. E-mail lopezjav@unican.es

NUMERICAL MODEL: IH-FOAM

Description

The numerical simulations of the present paper have been fulfilled with the model called IH-FOAM, see Higuera et al. (2013a, 2013b). This solver is based on OpenFOAM, a widely used open source CFD code.

It solves the three-dimensional Reynolds Averaged Navier-Stokes (RANS) equations for two incompressible phases using a finite volume discretization and the volume of fluid (VOF) method. In VOF, each phase is described by a fraction α occupied by the unit volume of water in the cell (0 means that the cell is full of air and 1 that it is full of water, being a mixture when in between). Its principal advantages are its simplicity, allowing very complex free surface configurations to be represented easily and that it involves no mesh motion, as VOF is advected. A minor disadvantage is that it becomes less effective when surface tension effects increase. However, we are dealing with relatively long wavelengths, so that only for very specific phenomena surface tension forces are not negligible.

IH-FOAM can also solve two-phase flow within porous media, solving the newly developed Volume-Averaged Reynolds-Averaged Navier-Stokes equations (VARANS, see del Jesus et al. (2012) for further details). The porous drag forces are modeled using the Forchheimer relationship. A k-ε turbulence model is used in both the clear fluid and the porous media flow region. It also supports automatically several turbulence models such as k-ω SST or LES, but no closure models are provided within the porous media.

On top of that, special boundary conditions which allow a simultaneous generation and active wave absorption of waves have been coded and added to the solver, so that it is now fully prepared to simulate all kinds of coastal engineering processes.

Governing Equations

The RANS equations, include continuity (1) and momentum conservation (2) equations. They are the governing mathematical expressions which describe the motion of fluid flow. The assumption of incompressible fluids has been used, which is applicable for most coastal engineering practical problems.

$$\nabla \cdot U = 0 \tag{1}$$

$$\frac{\partial \rho U}{\partial t} + \nabla \cdot (\rho U U) - \nabla \cdot (\mu_{\text{eff}} \nabla U) = -\nabla p^* - g \cdot X \nabla \rho + \nabla U \cdot \nabla \mu_{\text{eff}} + \sigma \kappa \nabla \alpha \tag{2}$$

ρ is the density, which is calculated as later presented in equation (3); U is the velocity vector; p^* is the excess in the hydrostatic pressure; g is the acceleration of gravity; X is the position vector. The last term on the right hand side of equation (2) is the effect of surface tension: σ is the surface tension coefficient; κ is the curvature of the interface and α is the indicator function, which has already been introduced, and will be further commented later in this section. Finally μ_{eff} is the efficient dynamic viscosity, which takes into account the molecular dynamic viscosity plus the turbulent effects: $\mu_{\text{eff}} = \mu + \rho \nu_{\text{turb}}$. The elements in equation (2) have a particular disposition: those placed on the left hand side of the equals sign are used in OpenFOAM to assemble the coefficient matrix, and the ones on the right side are calculated explicitly to form the independent term of the equations.

Using VOF it is straightforward to calculate any of the properties of the fluid at each cell, just by weighting them by the VOF value. For example, density of the cell is computed as follows:

$$\rho = \alpha \rho_{\text{water}} + (1 - \alpha) \rho_{\text{air}} \tag{3}$$

An additional equation must also be taken into account to describe the movement of the phases. The starting point for the equation which tracks the fluid movement is a classic advection equation, but as a sharp interface must be maintained and α must be conservative and bounded between 0 and 1, some restrictions apply. OpenFOAM makes use of an artificial compression term instead of using a compressing differencing scheme, as follows:

$$\frac{\partial \alpha}{\partial t} + \nabla \cdot U \alpha + \nabla \cdot U_c \alpha (1 - \alpha) = 0 \tag{4}$$

in which U_c is the compression velocity.

The boundedness of such equation is achieved by means of an especially designed solver called MULES (Multidimensional Universal Limiter for Explicit Solution). It makes use of a limiter factor on the fluxes of the discretized divergence term to ensure a final value between 0 and 1. For further reference regarding the governing equations see Rusche (2002).

Solving Procedure

Originally the solving algorithm for RANS was PISO (Pressure Implicit with Splitting of Operators), for a detailed description of the numerical solution of the equations see Kissling et al. (2010). More recent versions of the code have improvements. The new algorithm is called PIMPLE, as it is actually a mixture between PISO and SIMPLE (Semi-Implicit Method for Pressure-Linked Equations) algorithms. Both algorithms are thoroughly explained and applied for VOF in Jasak (1996). PIMPLE main structure is inherited from the original PISO, but it allows equation under-relaxation, as in SIMPLE, to ensure the convergence of all the equations at each time step.

A detailed flow chart, figure 4.1 in Higuera et al. (2013a), was developed in order to show the full loop for solving each time step.

Boundary Conditions

The only effort done in the wave generation and absorption field for OpenFOAM was recently presented in Jacobsen et al. (2011). Their approach is quite complete, accounting a great number of wave theories. However, they lack active wave absorption on the boundary, as they use relaxation zones. This technique has clear disadvantages as the existence of a wave damping region is known to produce an increment of the mean water level [Mendez et al. (2001)]. It also increases the computational domain by around two wave lengths [Wei and Kirby (1995)], which is quite inconvenient for already large domains and prototype applications. Another drawback is that each time step the waves are multiplied by a weighting function inside the relaxation zones, so if the time steps are very small and the simulations very long, the accuracy decreases due to machine precision errors.

To account for this lack, the boundary conditions in IH-FOAM include three dimensional regular waves generation as defined by Stokes I, II and V, cnoidal and stream function wave theories. Also first and second order directional irregular waves and Boussinesq solitary waves are supported. Full details are provided in Higuera et al. (2013a).

Active wave absorption has been implemented to work simultaneously with wave generation or independently. This feature is a key point for coastal engineering as it allows for longer simulations avoiding the increase of water level and agitation.

The 2D active absorption method is used as appears in Schäffer and Klopman (2000). It is the easiest technique to be implemented considering that it is based on linear shallow water theory (as presented in equation 5). Previous works on other numerical models Torres et al. (2010), Lara et al. (2011) have shown that it works relatively well even when used for waves outside the shallow water regime.

$$U\,h = c\,\eta \tag{5}$$

where U is horizontal velocity, h is the water depth, c is the wave celerity and η is the free surface elevation.

In order to cancel out the incident waves, the boundary must generate a velocity equal to the incident one but in the other direction. Therefore U can be assimilated to the correction velocity, and η with the value of the measured free surface. Since wave height is not known in advance, wave celerity can be approximated as follows: $c = \sqrt{g\,h}$. The active wave absorption expression is presented in equation 6.

$$U_c = -\sqrt{\frac{g}{h}}\eta_I \tag{6}$$

in which U_c is the correction velocity that is applied to a vector perpendicular to the boundary and pointing into the domain; and the incident wave height (η_I) is calculated by subtracting the measured

elevation at the wavemaker (η_M) from the target one (η_T), according to the expected reflection-free wave generation: $\eta_I = \eta_M - \eta_T$.

The practical application of the absorption theories to 3D consists in dividing the boundary in a given number of vertical elements, that we will call paddles due to the analogy with directional wavemakers.

NUMERICAL EXPERIMENTS

Mesh

Since the main objective was to test a breakwater at prototype scale, the domain has to be large enough to accommodate several wave lengths. A length of 270 m (X axis) and a width of 260 m (Y axis) are considered. The mesh height is 30 m, which ranges from the flat bottom to the top boundary, located 6.5 m over the crown wall, allowing for very large overtopping discharges. The initial resolution is 2 m in the horizontal directions, and 1 m in the vertical one.

The geometry of the vertical breakwater is presented in figure 1. A transversal section is presented in the left panel, and a plan view of the whole domain is shown in the right one. Note that the caisson lies on top of a porous foundation bed.
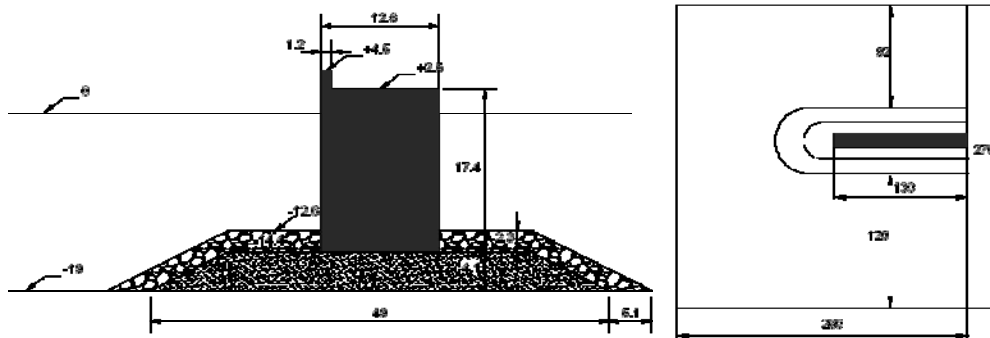

Figure 1. Geometry of the case. Left panel: section of the vertical breakwater. Right panel: plan view of the domain. Dimensions in meters.

The final mesh is around 3 million elements and is presented in figure 2. Within the base mesh the caissons and crown wall are removed using snappyHexMesh, refining the cells intersected by them once, obtaining double resolution up to a discretization of 1 m in the horizontal directions and 0.5 m in the vertical one. The same refinement process is carried out along the location of the free surface, which permits a better discretization of the propagating waves. This can be easily seen in figure 2.
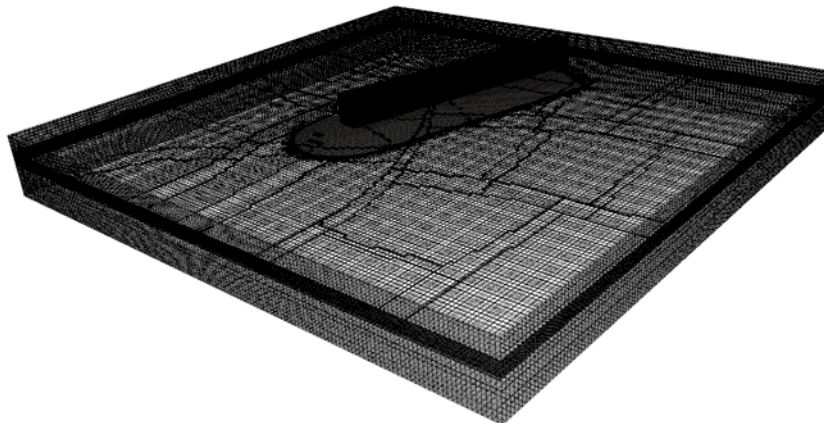

Figure 2. Final mesh. Note the greater resolution along the free surface and the angle between the generating boundary (right) and the breakwater.
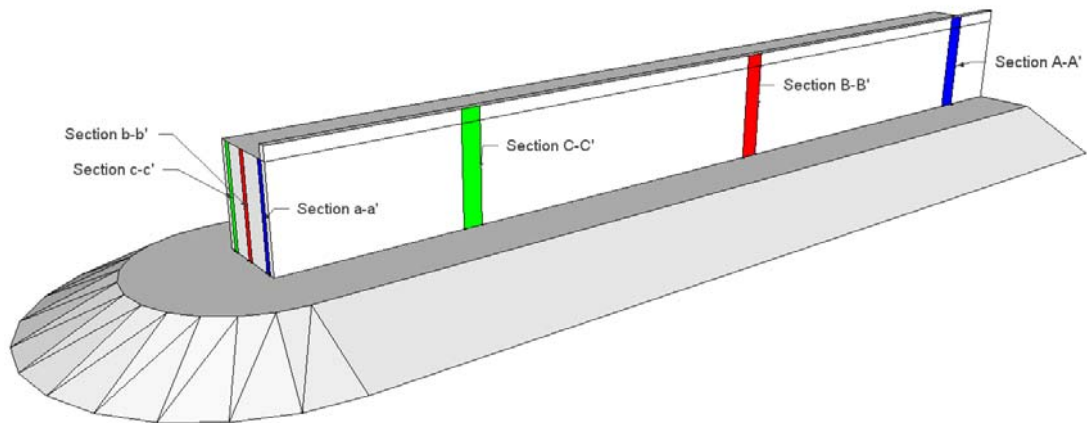
Figure 3. General view of the breakwater with the sampling sections.

Wave conditions

The still water level is set at 19 m. The structure is tested against a regular wave train of 6 m of wave height and 7 s of period, which was chosen in order to obtain large overtopping discharge events. The resultant wave length is 71.3 m, so that in front of the structure you can have 1.5 wave lengths.

The waves are generated using the cnoidal wave theory, and on top of it, active wave absorption is connected and applied to 65 individual elements.

Waves are always generated perpendicular to the boundary (0º incident angle). Directionality is obtained rotating the breakwater a certain angle (0º, 15º and 30º), and therefore, obtaining 3 different meshes which are equivalent in number of elements and discretization. Note that in figure 2 the breakwater is rotated 30º with respect to the right boundary.

Active wave absorption is also connected on the rest of boundaries (side boundary and rear end boundary), each of which has also 65 elements to absorb the incident waves.
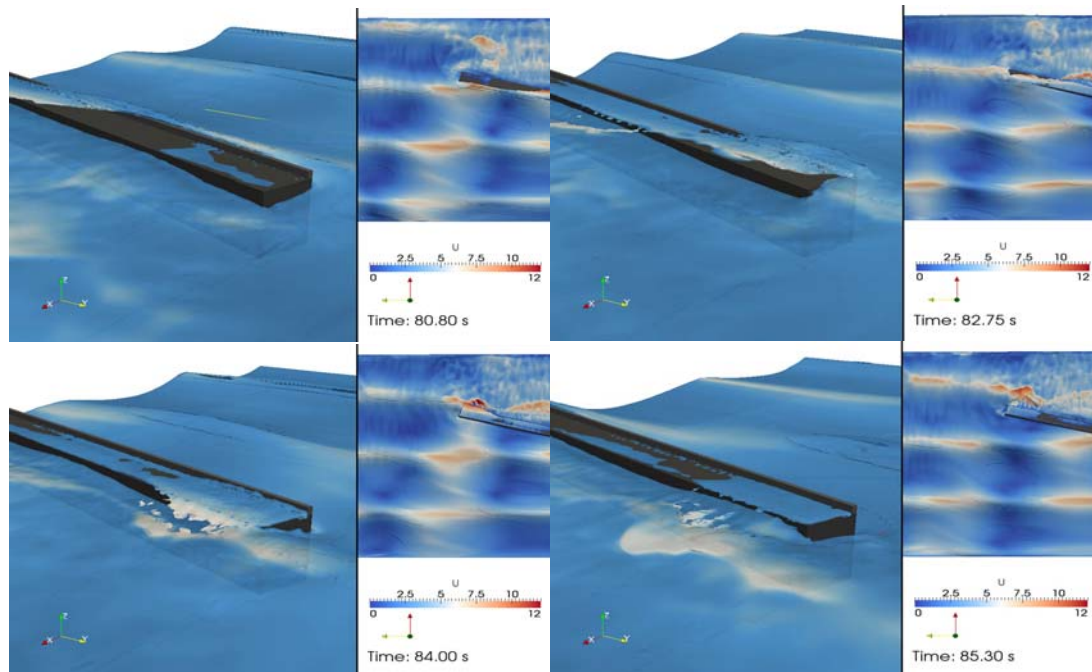

Figure 4. Snapshots of the simulations in four snapshots. Left panels: Detail of wave overtopping. Right view: Top view of the velocity field (in m/s) at the free surface.

RESULTS

Four snapshot of wave overtopping are presented in figure 4. Left panels present a side view of wave overtopping along the vertical breakwater. The four right panels display a top view of the wave field. Colored patterns represent velocity magnitude at the free surface.

Because of the obliqueness of the wave train, wave overtops the structure at the breakwater trunk to later overtop locations closer to the breakwater head. The layer of water, which passes over the breakwater crest, reaches the leeside part of the breakwater inducing wave breaking and generating wave oscillation. Moreover, part of the energy of the incoming wave train is also transmitted leeward due to wave diffraction at the breakwater head. Due to the use of active wave absorption boundaries, transmitted wave energy leaves the domain at the rear end boundary.

In front of the breakwater, a classical wave reflection pattern is observed. Nodes and antinodes can be detected at the different plots shown in figure 4. Velocity patterns plotted in red color show large velocity values corresponding to nodes and antinodes. Indeed, an antinode is located at the middle of the breakwater trunk, yielding a non-constant wave overtopping along the breakwater as it will be discussed latter. The model shows a very realistic wave field data and lays the foundation for the applicability of IH-FOAM to study three-dimensional wave fields around coastal structures.

Pressure

Results for pressure and overtopping discharge have been obtained and are presented in different sections of the breakwater, as represented by colors in figure 3.

Dynamic pressure results are shown in figures 5 and 6. Figure 5 corresponds to the pressure distribution in the front, back and bottom faces of the breakwater for the instant with a higher total force on them. The blue line corresponds to section A-A', the red line to section B-B', the green line to C-C' and the black line to Goda empyrical formulation. The top row corresponds to normal wave incidence (0º), the middle one to 15º and the bottom one to 30º.

We can note that for small angles of incidence, the blue and red lines show very similar results, not only between them, but also compared to Goda's formulation. Only a big difference appears in the top part of the seaside of the structure, and it is due to impulsive loading when overtopping occurs.

The green line is the closest to the breakwater head, and therefore, the one with higher influence of the three-dimensionality. This influence is easily observed, as for example, a wave trough is always located close to this section on the leeside part of the structure, so that dynamic pressure produces a great seaside net force. This fact also makes subpressures to be significantly smaller.

With respect to the front face (breakwater head), this zone is very relevant to study, as three dimensional structures generate in that specific place. Results are diplayed in figure 6. Also separation of the flow is expected, so that the challenge to obtain results in the zone is even greater, as there are no formulations available to study this effect.

These results (figure 6) show a great variability when accounting for both wave directionality and the location within the breakwater head. For the 0º incident angle, the wave crest is located near the blue section (a-a') while the green one (c-c') is closer to a small wave trough. Although they are barely 11 meters away there is a noticeable variation between the conditions due to the diffraction of the waves.

For the 30º incidence angle, all the sections have a higher level than the initial one, so they are all close to a wave trough.

The great variability between wave directions may be explained by the reflections, which can introduce a transversal oscillation in the tank, leading to a stationary system with nodes and antinodes. These effects shall be futher investigated in subsequent publications. Moerover the use of the active wave absorption at all the boundaries allows to get a stationary wave field in front of the breakwater.
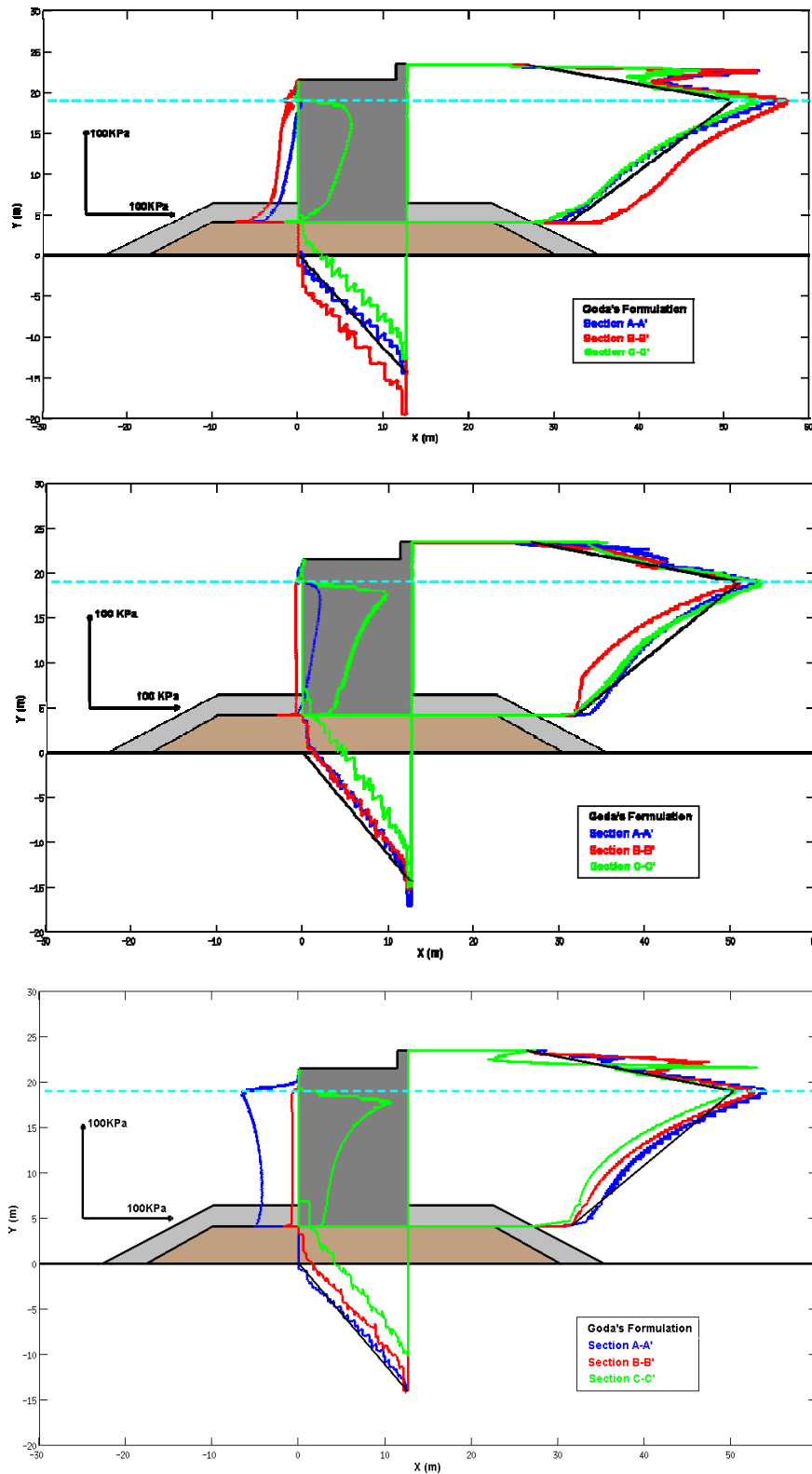
Figure 5. Dynamic pressure distribution along the lateral wall sections A, B and C. 0⁰ incidence for the top row. 15⁰ incidence angle for the middle row. 30⁰ incidence angle for the bottom row.
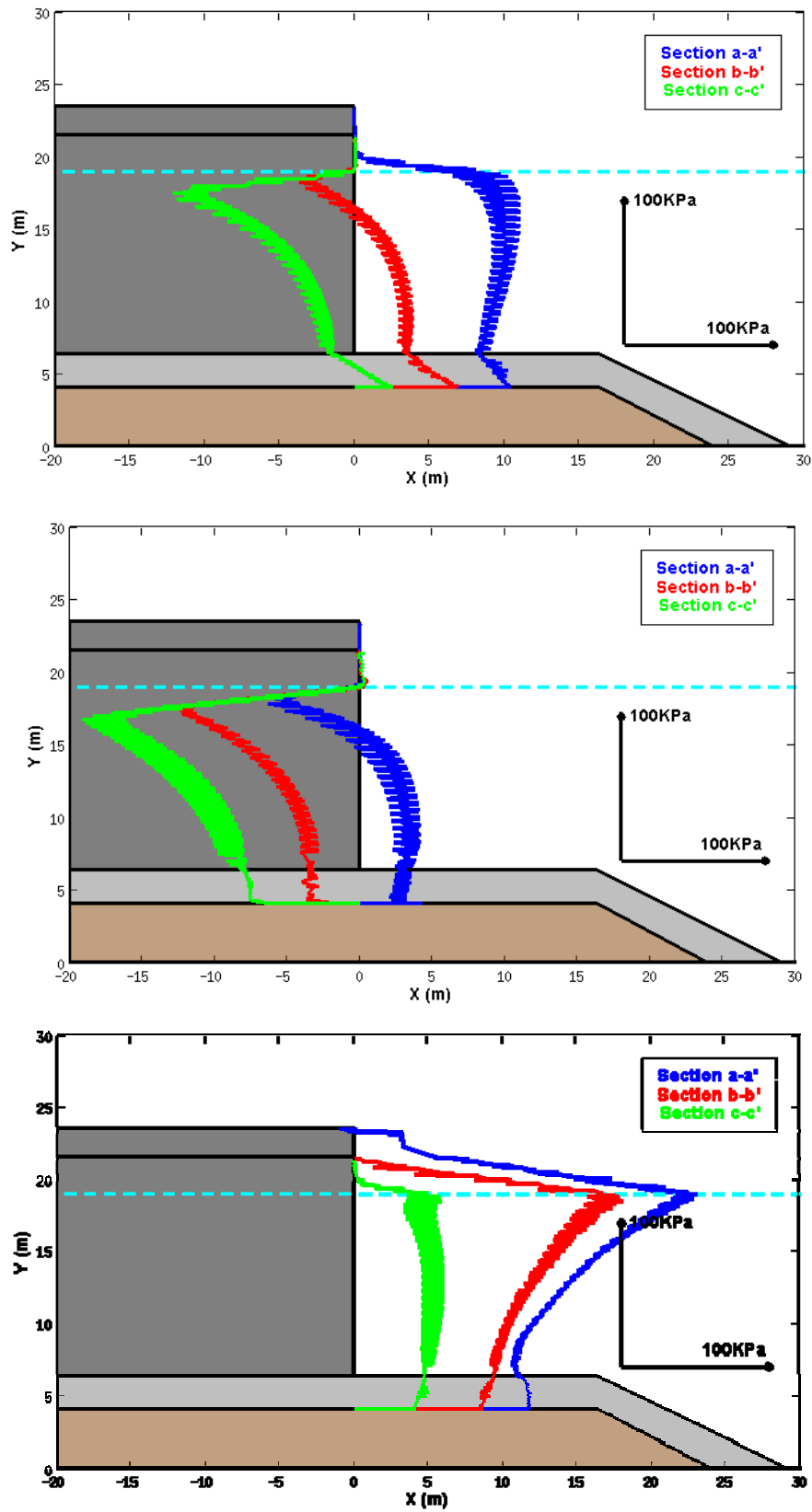
Figure 6. Dynamic pressure distribution along the breakwater head sections a, b and c for the right column. 0⁰ incidence for the top row. 15⁰ incidence angle for the middle row. 30⁰ incidence angle for the bottom row.

Overtopping

Overtopping results are preliminary, and are presented in figure 7. The horizontal axis corresponds to distance on the breakwater from the breakwater starting point near the wall towards the breakwater head. In this figure the colors no longer indicate section, but the incidence angle of the waves as noted in the legend. The horizontal black line is the theoretical result for the mean overtopping discharge given in the Overtopping Manual.

The normal incident waves (blue color) show a good agreement with the Overtopping Manual near both ends but it is highly overestimated in the central section. This may once again be caused by the transversal stationary wave, which gets an antinode close to the mid point of the breakwater.

A similar situation occurs for the waves with higher incident angles: the overtopping in the middle section is highly overestimated. However, the most relevant fact is that overtopping near the breakwater head increases by a great factor (more than 2 in both cases), especially for the 15º incident waves.
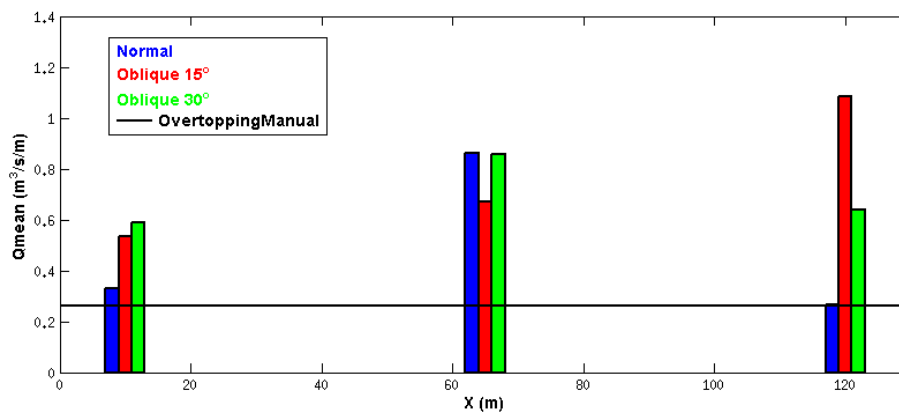

Figure 7. Mean overtopping discharge

CONCLUSIONS

Over the last years Navier-Stokes numerical models have been developed to accurately simulate wave interaction with all kinds of coastal structures, focusing on both functionality and stability of coastal structures. Although several models have been used to simulate wave interaction with coastal structures in two dimensions (2DV) there are a vast number of three-dimensional effects that need to be investigated in order to improve the design. In this paper a new model called IH-FOAM has been applied to study a vertical breakwater at prototype scale. As a first attempt of validation, the model has been used to simulate a regular wave train generated with a relative angle with the breakwater, inducing three-dimensional wave pattern not only seaward the structure due to reflection but also generating an overtopping discharge variation along the breakwater trunk.

Pressure laws and overtopping discharge at three different cross-sections along the structure have been studied. Pressure laws have been compared with classical Goda's formulation. Although, the numerical model predictions are in accordance with Goda's calculations, a clear three-dimensional variability of wave-induced pressure has been observed. Moreover, an additional study has been performed calculating pressure laws at the side-wall on the breakwater head. Large three-dimensional effects are detected from the simulations due to the flow separation at that area.

Overtopping model predictions have been compared with Overtopping Manual calculations showing very close values along the trunk. However, lower overtopping discharge values are observed at the breakwater head.

This paper is a preliminary work to show the range of applicability of a three-dimensional Navier-Stokes model to study wave interaction with a vertical breakwater under the action of an oblique wave train.

REFERENCES

del Jesus, M., Lara, J.L., Losada, I.J., 2012. Three-dimensional interaction of waves and porous coastal structures. Part I: Numerical model formulation. *Coastal Engineering*. 64, 57–72.

Guanche, R., I.J. Losada and J.L. Lara. (2009). Numerical analysis of wave loads for coastal structure stability, *Coastal Engineering, ELSEVIER*, vol. 56, 543-558

Higuera, P., Lara, J.L., Losada, I.J. (2013a In Press). Realistic wave generation and active wave absorption for Navier–Stokes models. Application to OpenFOAM. *Coastal Engineering.* http://dx.doi.org/10.1016/j.coastaleng.2012.07.002

Higuera, P., Lara, J.L., Losada, I.J. (2013b In Press) Simulating Coastal Engineering Processes with OpenFOAM. *Coastal Engineering.* http://dx.doi.org/10.1016/j.coastaleng.2012.06.002

Jacobsen, N.G., Fuhrman, D.R. and Fredsøe, J. (In Print) A wave generation toolbox for the open-source CFD library: OpenFoam. *International Journal for Numerical Methods in Fluids.*

Jasak, H. (1996). Error analysis and estimation for the finite volume method with applications to fluid flows. *PhD thesis*, Imperial College of Science, Technology and Medicine.

Kissling, K., Springer, J., Jasak, H., Schütz, S., Urban, K., and Piesche, M. (2010). A coupled pressure based solution algorithm based on the volume-of-fluid approach for two or more immiscible fluids. *V European Conference on Computational Fluid Dynamics, ECCOMAS CFD.*

Lara, J.L., Losada, I.J., Guanche, R., 2008. Wave interaction with low-mound breakwaters using a RANS model. *Ocean Engineering* 35 (13), 1388–1400.

Lara, J.L., Ruju, A. and Losada, I.J. (2011) Reynolds Averaged Navier-Stokes modelling of long waves induced by a transient wave group on a beach. Proceedings of the Royal Society A, vol. 467, 1215-1242.

Lara, J.L., del Jesus, M., Losada, I.J., 2012. Three-dimensional interaction of waves and porous coastal structures. Part II: Experimental validation. *Coastal Engineering* 64, pp. 26–46.

Losada, I.J., Lara, J.L., Guanche, R., Gonzalez-Ondina, J.M. (2008). Numerical analysis of wave overtopping of rubble mound breakwaters. *Coastal Engineering*, vol 55 (1), pp. 47-62.

Mendez, F.J., Losada, I.J. and Losada, M.A. (2001) Wave-induced mean magnitudes in permeable submerged breakwaters. *Journal of Waterway, Port, Coastal and Ocean Engineering*, vol. 127, 7-15.

Rusche, H., 2002. Computational fluid dynamics of dispersed two-phase flows at high phase fractions. *Ph.D. thesis*, Department of Mechanical Engineering, Imperial College of Science, Technology & Medicine, London.

Schäffer, H.A. and Klopman, G. (2000) Review of multidirectional active wave absorption methods. *Journal of Waterway, Port, Coastal and Ocean Engineering*, March/April, 88-97.

Torres-Freyermuth, A., Lara, J.L. and Losada, I.J. (2010) Numerical modelling of short and long-wave transformation on a barred beach. *Coastal Engineering*, vol. 57, 317-330.

Wei, G. and Kirby, J.T. (1995) Time-dependent numerical code for extended Boussinesq equations. *Journal of Waterway, Port, Coastal and Ocean Engineering*, vol. 121 (5), 251-261.